Journal of Petroleum Science and Engineering 206 (2021) 109038

Contents lists available at ScienceDirect

Journal of Petroleum Science and Engineering

journal homepage: www.elsevier.com/locate/petrol

Optimization of WAG in real geological field using rigorous soft computing techniques and nature-inspired algorithms

Menad Nait Amar [a,b], Ashkan Jahanbani Ghahfarokhi [c,*], Cuthbert Shang Wui Ng [c], Noureddine Zeraibi [b]

[a] Département Etudes Thermodynamiques, Division Laboratoires, Sonatrach, Avenue 1er Novembre, 35000, Boumerdes, Algeria
[b] Laboratory of Hydrocarbons Physical Engineering, Faculty of Hydrocarbons and Chemistry, University of M'Hamed Bougara Boumerdes, Avenue 1er Novembre, 35000, Boumerdes, Algeria
[c] Department of Geoscience and Petroleum, Norwegian University of Science and Technology, S. P. Andersens Veg 15b, 7031, Trondheim, Norway

ARTICLE INFO

Keywords:
Water alternating gas (WAG)
Enhanced oil recovery (EOR)
Machine learning
Nature-inspired algorithms
Constraints handling

ABSTRACT

To meet the ever-increasing global energy demands, it is more necessary than ever to ensure increments in the recovery factors (RF) associated with oil reservoirs. Owing to this challenge, enhanced oil recovery (EOR) techniques are increasingly gaining more significance as robust strategies for producing more oil volumes from mature reservoirs. Water alternating gas (WAG) injection is an EOR method intended at improving the microscopic and macroscopic displacement efficiencies. To handle and implement successfully this technique, it is of vital importance to optimize its operating parameters. This study targeted at implementing robust proxy paradigms for investigating the suitable design parameters of a WAG project applied to real field data from "Gullfaks" in the North Sea. The proxy models aimed at reducing significantly the rum-time related to the commercial simulators without scarifying the accuracy. To this end, machine learning (ML) approaches, including multi-layer perceptron (MLP) and radial basis function neural network (RBFNN) were implemented for estimating the needed parameters for the formulated optimization problem. To improve the reliability of these ML methods, they were evolved using optimization algorithms, namely Levenberg–Marquardt (LM) for MLP, and ant colony optimization (ACO) and grey wolf optimization (GWO) for RBFNN. The performance analysis of the proxy models revealed that MLP-LMA has better prediction ability than the other two proxy paradigms. In this context, the highest average absolute relative deviation noticed per runs by MLP-LMA was lower than 3.60%. Besides, the best-implemented proxy was coupled with ACO and GWO for resolving the studied WAG optimization problem. The findings revealed that the suggested proxies are cheap, accurate, and practical in emulating the performance of numerical reservoir model. In addition, the results demonstrated the effectiveness of ACO and GWO in optimizing the parameters of WAG process for the real field data used in this study.

1. Introduction

Since the dawn of the 21st century, the population growth and the enormous advancements of industry have created an acute need for energy (Tillerson, 2008). Despite all the efforts to replace fossil fuels with other energy sources, they still remain the most used and demanding source of energy. As oil reservoirs that were easy to locate and operate are increasingly moving towards the vision of scarcity, the main challenge and current interest is to better exploit the proven reservoirs by acting on the reservoir and its effluents (Ahmadi et al., 2018).

The production cycle from the oil reservoirs passes through three recovery phases: primary, secondary and tertiary, depending on the driving forces and the drainage mechanisms involved in the production (Ahmed, 2018). During primary recovery, these come from the natural energy source associated with the rock and fluids in the reservoir. Secondary recovery processes are often implemented in the presence of aquifer or/and gas cap by injecting respectively water and gas into these sources. This kind of injection allows maintaining the pressure of reservoir in a manner such that the production increases. Since the recovery factors provided by primary and secondary methods do not usually reach high values, applying tertiary recovery techniques known as enhanced oil recovery (EOR) has become a necessity (Ahmadi and

* Corresponding author.
E-mail address: ashkan.jahanbani@ntnu.no (A. Jahanbani Ghahfarokhi).

https://doi.org/10.1016/j.petrol.2021.109038
Received 6 February 2021; Received in revised form 25 April 2021; Accepted 18 May 2021
Available online 7 June 2021

Shadizadeh, 2013; Lake et al., 2014).

Currently, water alternating gas (WAG) injection in its two main forms, i.e., immiscible and miscible, is one of the most used EOR methods due to its efficiency and simplicity of implementation (Afzali et al, 2018, 2020; Kulkarni and Rao, 2005; Ranaee et al., 2019). Besides, this technique has the advantages of the two conventional assisted recovery methods, which are water injection and gas injection. The implementation and management of WAG process consists of optimizing the influencing factors of this EOR method in order to establish the best strategies to maximize the recovery factor (Christensen et al., 2001; Nait Amar et al., 2018a). Numerical simulation is usually the standard decision-making tool used in the industry for this workflow.

While investigating the proper operating parameters of a WAG process, it is quite often to confront the dichotomy relating precision to calculability efforts of a model: on one side, the latter must meet the precision requirements, and on the other, it must be fast enough to meet the practical needs. In addition, the optimization task is very complex, because significant number of scenarios must be evaluated, and each evaluation requires the execution of a time-consuming run. Due to the non-linearity and complexity of the problem under consideration, leading to intensive computing and significant CPU times, the development of robust alternative tools capable of keeping the complexity of the reservoir model and reducing the execution time is necessary, as shown in our prior works (Nait Amar et al, 2018a, 2020b; Nait Amar and Zeraibi, 2019).

In recent years, there has been growing recognition of the vital link between handling complex systems and soft computing (SC) approaches (Zendehboudi et al., 2018). Indeed, these approaches are increasingly playing central role in addressing the issues of calculability and reliability in different fields. Various published studies have witnessed the successful implementation of SC techniques in resolving complicated systems and modelling high-complexity phenomena such as flow assurance problems (Benamara et al., 2020; Hemmati-Sarapardeh et al., 2013, 2019, Nait Amar, 2021; Nait Amar et al., 2021), estimating parameters related to the oil and gas industry (Baldwin et al., 1990; Ghiasi et al., 2014; Ghiasi and Mohammadi, 2015; Kamari et al., 2014; Zendehboudi et al., 2018), and CO_2 utilization related parameters (Amooie et al., 2019; Bakyani et al., 2016; Daryasafar et al., 2019; Hemmati--Sarapardeh et al., 2016; Rashid et al., 2017).

Regarding the alternative approaches suggested in the literature for optimizing the WAG processes, Panjalizadeh et al. (2015) applied a surface response methodology for investigating the suitable parameters of a WAG process in an inverted five-spot pattern. The authors combined polynomial regression techniques, namely quadratic and cubic schemes, with some classical sampling strategies for implementing their workflow. Jaber et al. (2017) suggested a proxy model gained by generating CO_2-WAG scenarios using Box-Behnken design and performing quadratic regression. Zhang et al. (2017) established a reliable approach consisted of a combination of two algorithms, namely steepest ascent and simplex stochastic gradient, to investigate the best well trajectories and controls that allow maximizing the net present value (NPV) for a water/surfactant solution and CO_2 gas (WAG/SAG) process. Mohaghegian et al. (2018) considered robust evolutionary algorithms, including particle swarm optimization (PSO) and genetic algorithm (GA), for the automatic optimization of the WAG process Norne field, specifically the E-segment. In their approach, NPV was the objective function. Nait Amar et al. (2018a) implemented dynamic proxy models of a compositional reservoir and coupled these proxies with 2 different metaheuristic algorithms, namely GA and ant colony optimization (ACO), to conduct the optimization of WAG. In another approach, Nwachukwu et al. (2018) employed the extreme gradient boosting (XGBoost) to develop the proxies and used Mesh Adaptive Direct Search (MADS) to optimize well locations and parameters of a WAG process under geological uncertainty. More intriguingly, Nait Amar and Zeraibi (2019) coupled their developed dynamic proxy with Non-Dominated Sorting Genetic Algorithm version II (NSGA-II) to conduct the multi-criteria optimization of WAG CO_2 injection. In addition to this, Belazreg et al. (2019) illustrated novelty by using group method of data handling (GMDH) to develop the predictive model of WAG incremental recovery factor based on the data from a reservoir model. Thereafter, Belazreg and Mahmood (2020) demonstrated the practicality of GMDH in the predictive proxy development by using the real field data from worldwide WAG pilot projects (28 cases). Moreover, Belazreg et al. (2020) showed that random forest algorithm could also be applied to forecast the increasing in the recovery factor of CO_2 WAG process. In the same context, Nait Amar et al. (2020b) evolved support vector regression (SVR) using GA to establish a dynamic proxy and implemented GA along with this proxy to optimize WAG CO_2 process. Also, Yousef et al. (2020) used the methodology of top-down modelling, which was coined by Mohaghegh (2017), to build a model that could predict the reservoir performance of a carbonate onshore in Middle East under WAG process. The literature survey on the application of intelligent proxies for predictive analysis in WAG process reveals the high ability of these advanced schemes for dealing with different formulated optimization problems.

In the present study, reliable proxy models were proposed to optimize the design parameters of a WAG process in a real field, “Gullfaks” in the North Sea. The task was formulated as a constrained non-linear problem. Two artificial neural network types, viz. multilayer perceptron (MLP) and radial basis function neural network (RBFNN), were implemented to model the different parameters needed in the optimization problem. Levenberg–Marquardt algorithm (LMA) was the learning algorithm for the MLP model, while ant colony optimization (ACO) and grey wolf optimization (GWO) were implemented for optimizing the RBFNN control parameters. After confirming the accuracy of different proxy models, the best performing one was coupled with ACO and GWO to identify the proper design parameters of the studied WAG optimization problem. The main contribution of this work can be summarized as establishing new smart hybridization, soft-computing techniques and nature-inspired algorithm, for developing robust proxy models that can deal with real geological fields when implementing EOR techniques such as WAG, thus, avoiding performing a great number of direct time-consuming reservoir simulation runs.

2. Methods

2.1. Modelling techniques

Artificial neural network (ANN) is a robust type of machine learning techniques, which has a great ability for recognizing patterns and distinguishing relationships regardless the complexity and the non-linearity of a given system (Haykin, 2010; Nait Amar et al., 2020a). The conception and the functioning of ANN are inspired from the human brain and its learning processes. The topology of an ANN model involves mainly the neurons which are known also as nodes (Varamesh et al., 2017a). The neurons are allocated to three kinds of layers:

- Input layer: It is the first layer in the paradigm. It receives the inputs, and hence its number of neurons is similar to the dimensionality of the system.

- Output layer: It corresponds to the last layer in the network. It allows to gain the outcomes of the network. Its number of neurons represents the number of outputs of the system.
- Hidden layer(s): This type is known as intermediate layer(s) as they are between the input and output layers. The principal role of this kind is to alter the data by mapping them in higher dimensionality features to capture the non-linearity of the system.

The structure of an ANN is characterized by another vital parameter, the weights, which ensure the connection between the neurons of two succeeding layers. Besides, the neurons of the hidden and output layers include bias terms.

Different types of ANN can be distinguished according to the topology schemes and the manner of treating or learning the information. In this context, multilayer perceptron (MLP) and radial basis function neural network (RBFNN) are two robust types (Karkevandi-Talkhooncheh et al., 2018; Siddique and Adeli, 2013):

- Multilayer perceptron (MLP): this type of ANN involves at least one hidden layer (Haykin, 2010). Several activation functions, such as logsig and tansig are frequently applied in the hidden layers to map the inputs in a non-linear feature. The number of hidden layers and their neurons as well as their activation function are determined by means of trial and error method (Varamesh et al., 2017b). The learning stage of an MLP aims at achieving the proper weight and bias values. To do so, several back-propagation algorithms can be applied. In this investigation, Levenberg–Marquardt algorithm (LMA) was implemented in the learning phase of MLP paradigm. More information about this technique can be found in prior works, e.g. (Haykin, 2010; Hemmati-Sarapardeh et al., 2018).
- Radial basis function neural network (RBFNN): It covers only one hidden layer. In the nodes of this hidden layer, a radial basis function is applied as a kind of non-linear transformation (Tatar et al, 2015, 2016; Zhao et al., 2015). Gaussian function is the frequently applied RBF characterized by it spread coefficient (σ^2). To ensure reliable performance of a RBFNN model, the number of hidden nodes and the spread coefficient of the Gaussian function should be determined properly. In this study, we have applied two metaheuristic algorithms, namely ant colony optimization (ACO) and grey wolf optimization (GWO), to optimize these control parameters.

2.2. Optimization algorithms

2.2.1. Ant colony optimization (ACO)

Ant Colony Optimization (ACO) is another reliable nature-inspired optimization algorithm. ACO mimics the real-searching process applied by ants for food searching (Blum, 2005). Like the other nature-inspired algorithms, ACO applies two principles: exploration (investigating new parts of the search space) and exploitation (improving the existing solutions). These processes are facilitated by the mechanism of depositing pheromone with different concentrations. These concentrations are proportional to the quantity and the quality of food (Hemmati Sarapardeh et al., 2020). Accordingly, the pathway with the highest concentration will be the shortest and will be followed by the maximum number of ants.

The adaptation of the real-ant principle is given as per following steps (Heris and Khaloozadeh, 2014; Socha and Dorigo, 2008):

- Initialization: an initial population m of ants is created randomly in the search space.
- Evaluation: a fitness function is included as an assessment indexes for the individuals.
- Solution archive: sorting the ants from best to worst according to the fitness function.
- Weight application: solution archive members are provided with weight values w_i. The following equation is therefore applied (Hemmati Sarapardeh et al., 2020; Heris and Khaloozadeh, 2014; Socha and Dorigo, 2008):

$$w_i \propto \frac{1}{\sqrt{2\pi}\alpha m}\exp\left[-\frac{1}{2}\left(\frac{i-1}{\alpha m}\right)^2\right] \tag{1}$$

$$\sum_{i=1}^{m} w_i = 1 \tag{2}$$

Equation (1) sets the weight values to be distributed under a Gaussian function with element indexes 'i', mean value of 1, and standard deviation αm, where α is a parameter of the algorithm and m is the number of ants.

- Probabilistic paradigm: this model based on the Gaussian mixture is applied as shown below (Hemmati Sarapardeh et al., 2020; Heris and Khaloozadeh, 2014):

$$G^n(x[n]) = \sum_{i=1}^{m} w_i N(x[n]; \mu_i[n],\ \sigma_i[n]) \tag{3}$$

$$N(x; \mu,\ \backslash\sigma) = \frac{1}{\sqrt{2\pi}\sigma}\exp\left[-\frac{1}{2}\left(\frac{x-\mu}{\sigma}\right)^2\right] \tag{4}$$

In the above equation, n is the index number and $x[n]$ corresponds to the nth element in vector x.

Then, the mean (μ) and standard deviation of the Gaussian mixture (σ) are calculated as (Hemmati Sarapardeh et al., 2020):

$$\mu_i[n] = x_i[n] \tag{5}$$

$$\sigma_i[n] = \frac{\delta}{m-1}\sum_{i'=1}^{m}[x_i[n] - x_{i'}[n]] \tag{6}$$

The positive parameter δ is a factor for balancing between the exploitation and exploration.

- Sampling: a predefined number of new individuals is gained based on the archive outcomes.
- Selection: the fittest elements and the new offspring are exploited to generate a new archive.
- The best solution is the fittest individual in the archive.

These steps are repeated until the satisfaction of a stopping criterion.

2.2.2. Grey wolf optimization (GWO)

Grey wolf optimizer (GWO) is another example of metaheuristic optimization techniques which was initiated by Mirjalili et al., (2014). This algorithm has been significantly applied in the petroleum industry as discussed in several literature (Bian et al, 2018, 2019, 2020; Nait Amar et al., 2018b) thanks to its robustness and simple implementation. Fundamentally, it is inspired by the natural hierarchy of leadership and hunting habit of grey wolves (Mirjalili et al., 2014). Regarding the optimization mechanism of GWO, the population of grey wolves can be categorized into four different groups, namely alpha (α), beta (β), delta (δ), and omega (ω). According to the ranking of the social leadership, α wolves are considered the highest among others and then, they are followed by β, δ, and ω wolves. Mathematically, a population of wolves is represented as a set of random solutions which is evaluated by using a predefined objective function to compute its respective fitness value (Hemmati Sarapardeh et al., 2020). Thereafter, the categorization of wolves' population into the four above-mentioned groups is done based on the assessed fitness value. During the optimization process, the three best wolves: α, β, and δ, would gradually lead the other ω wolves towards the prey, which is the global optimum, in the search space. This can be done by updating the wolves' positions as follows (Mirjalili et al., 2014):

Table 1
Description of the numerical model (Shpak, 2013).

Parameters	Value	Unit
Top of the reservoir	1870	m
Reservoir temperature	71.1	°C
Initial reservoir pressure, P_i	320	bar
GOR (in-situ)	102	sm^3/sm^3
Formation volume factor at P_i	1.254	rm^3/sm^3
Oil density	617.2	Kg/m^3
Oil viscosity	0.203–0.260	cP
Permeability	0.4–4	D
Porosity	20–35	%
Compressibility of the rock at P_i	9×10^{-5}	bar^{-1}
Initial oil in place	19.7×10^6	sm^3
Total number of grids	57,375 ($45 \times 75 \times 17$)	/
EOS	Peng-Robinson	/
Number of producer wells	3	/
Number of injector wells	3	/

Table 2
Compositions of the reservoir fluid and injection gas.

Composition	Molar fractions of the reservoir fluid (%)	Molar fractions of the injection gas (%)
C1	50	77
C3	3	20
C6	7	3
C10	20	0
C15	15	0
C20+	5	0

$$\vec{D} = \left| \vec{C} . \vec{X_p}(t) - \vec{X}(t) \right| \tag{7}$$

$$\vec{X}(t+1) = \left| \vec{X_p}(t) - \vec{A} . \vec{D} \right| \tag{8}$$

$$\vec{A} = 2\vec{a} . \vec{r_1} - \vec{a} \tag{9}$$

$$\vec{C} = 2\vec{r_2} \tag{10}$$

where t represents the current step of iteration, $\vec{X}$ denotes the position vector of a grey wolf, $\vec{X_p}$ indicates the position vector of the prey, $\vec{a}$ is generally reduced from 2 to 0, and $\vec{r_1}$, $\vec{r_2}$ act as the random vectors between 0 and 1. In the algorithm of GWO, the position vector of the prey (optimum) is unknown. Therefore, it is expected that the position vectors of α, β, and δ are treated as the optimum. Thereafter, the other ω wolves will re-adjust their positions with respect to those of α, β, and δ as shown below (Mirjalili et al., 2014):

$$\vec{D_\alpha} = \left| \vec{C_1} . \vec{X_\alpha}(t) - \vec{X}(t) \right| \tag{11}$$

$$\vec{D_\beta} = \left| \vec{C_2} . \vec{X_\beta}(t) - \vec{X}(t) \right| \tag{12}$$

$$\vec{D_\delta} = \left| \vec{C_3} . \vec{X_\delta}(t) - \vec{X}(t) \right| \tag{13}$$

where $\vec{X_\alpha}(t)$ means the position vector of α wolves at iteration t, $\vec{X_\beta}(t)$ points out the position vector of β wolves at iteration t, and $\vec{X_\delta}(t)$ shows the position vector of δ wolves at iteration t, and $\vec{X}(t)$ is the position vector of the current best solution. Basically, the above equations are used to approximate the distance between the current solution and α, β, and δ wolves (Mirjalili et al., 2014):

$$\vec{X_1} = \left| \vec{X_\alpha}(t) - \vec{A_1} . \vec{D_\alpha} \right| \tag{14}$$

$$\vec{X_2} = \left| \vec{X_\beta}(t) - \vec{A_2} . \vec{D_\beta} \right| \tag{15}$$

$$\vec{X_3} = \left| \vec{X_\delta}(t) - \vec{A_3} . \vec{D_\delta} \right| \tag{16}$$

After that, the final position of the current solution is computed based on the following equation (Mirjalili et al., 2014):

$$\vec{X_{(t+1)}} = \frac{\vec{X_1} + \vec{X_2} + \vec{X_3}}{3} \tag{17}$$

The steps described above are repeated until the fulfilment of a stopping criterion.

3. Description of the reservoir model

The segment K1/K2 is a part of Gullfaks reservoir. This segment has an average thickness of 200 m and its top is at 1870 m. The K1/K2 segment is sandstone and is characterized by excellent permeability values (Shpak, 2013).

The reservoir is not supported by either an aquifer or a gas cap. Six wells are located in this segment (3 producers and 3 injectors). The year 2016 is assumed to be the start of production, 2018 is assumed to be the implementation time of the WAG process and the year 2026 is the end of the simulations. The description of the numerical model of K1/K2 segment is shown in Table 1. The compositions of the reservoir fluid and the injected gas are stated in Table 2. The compositions considered are taken from the SPE5 comparative study model (Killough et al., 1987).

The distribution of the petrophysical characteristics, the position of the faults, and the location of the wells in the reservoir are illustrated in Fig. 1.

In this investigation, a numerical slim-tube model consisted of a one-dimensional compositional paradigm (in Eclipse 300) was considered to estimate the minimum miscibility pressure (MMP) of the injected gas. The latter is defined as the lowest pressure at which multi-contact miscibility between the reservoir fluid and the injected gas can be reached. The length and the width of the model are equal to 100 m and 1 cm, respectively. This paradigm covers 600 grids with permeability and porosity of 2000 mD and 10%, respectively. The injection well was located at the first grid of the model (1,1,1), while the production well was placed at the end grid of the model (600,1,1). Whitson et al. (2000) proposed that the MMP corresponds to the pressure at which the recovery factor is ~0.95 after injecting 1.2 pore volumes (PV) of gas. To estimate the MMP value, the gas is injected at various pressure values and the achieved recovery factor is reported after injecting 1.2 PV gas. According to the results, the MMP of the injected gas is about 199.6 bar which is below the initial reservoir pressure, so the type of the WAG in this study is miscible.

4. Problem formulation

Field oil production total (FOPT) is assumed the objective function to optimize during the implementation of the WAG process. In addition, two dynamic technical constraints are specified as follows:

- A limit of 50% for daily water cut (Field Water Cut: FWCT).
- The reservoir pressure must be higher than the MMP value.

The considered design parameters are summarized in Table 3. The half-cycle time is defined as the time period during which the gas/water is continuously injected. The downtime parameter corresponds to the number of years in which the WAG process is active; in other words, after this time, the production is mainly by water injection until the end of the simulation (2026). Based on the minimum and maximum values of this parameter, three levels were considered (3, 4 and 5 years) to differentiate the time stages of the WAG, namely:

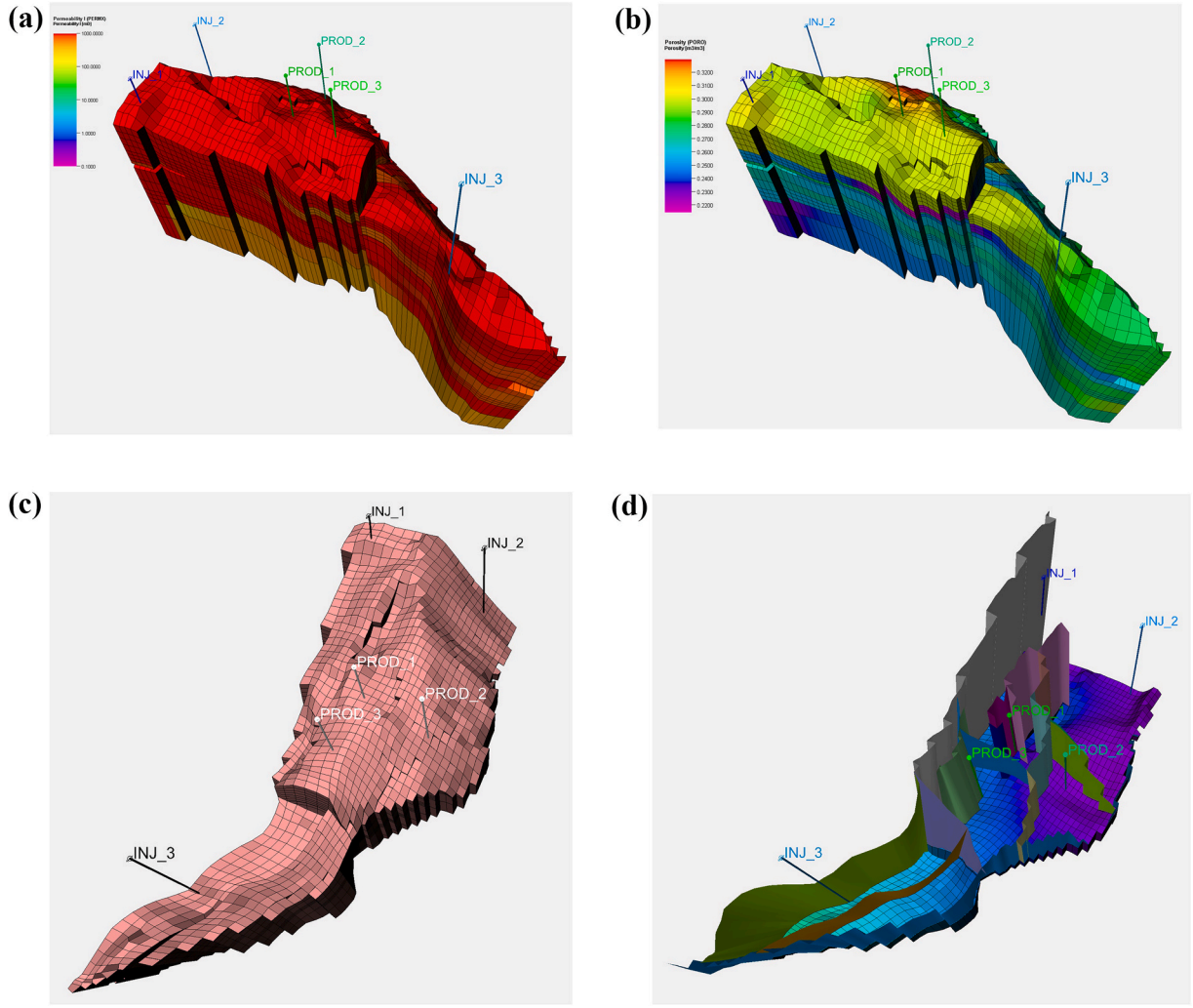

Fig. 1. Illustration of the main characteristics of the segment K1/K2: (a) permeability distribution; (b) porosity distribution; (c) well locations; (d) fault positions (Shpak, 2013).

Table 3
The considered WAG design parameters.

Parameter	Min	Max
Water injection rate: q_{injw} (sm^3/d)	2000	6000
Gas injection rate: q_{injg} $(10^6 sm^3/d)$	1.0	2.1
Half-cycle time: $half_{cycg-w}$(months)	3	12
Downtime (years)	3	5

Table 4
The considered control parameters for ACO and GWO.

Algorithm	Parameters	Value
ACO	Population size	60
	Archive Size	60
	Selection probability	0.5
	Max number of generations	50
GWO	Number of wolves	60
	Max number of iterations	60
	a (linear decreasing)	2 to 0

- Late time: 5 years.
- Middle time: 4 years.
- Early time: 3 years.

Water and gas injection rates are used to determine the WAG ratio. Gas injection rate over half-cycle time gives the slug size.

The optimization problem (P) is formulated as follows:

$$(P): \begin{cases} \text{maximize } FOPT\left(q_{injw}, q_{injg}, half_{cycg-w}, downtime\right) \\ subject\ to \\ 2000\dfrac{sm^3}{d} \le q_{injw} \le 6000\dfrac{sm^3}{d} \\ 1\times10^6\dfrac{sm^3}{d} \le q_{injg} \le 2.1\times10^6\dfrac{sm^3}{d} \\ 3\ months \le half_{cycg-w} \le 12\ months \\ Downtime \in \{3,4,5\}_{years} \\ MMP \le FPR\left(t, q_{injw}, q_{injg}, half_{cycg-w}, downtime\right) \\ FWCT\left(t, q_{injw}, q_{injg}, half_{cycg-w}, downtime\right) < 50\% \end{cases} \tag{18}$$

where t is the time, FOPT is the field oil production total, q_{injw} and q_{injg} represent the field water and gas injection rates, respectively, FPR is the field pressure, and FWCT is the field water cut which is expressed as follows:

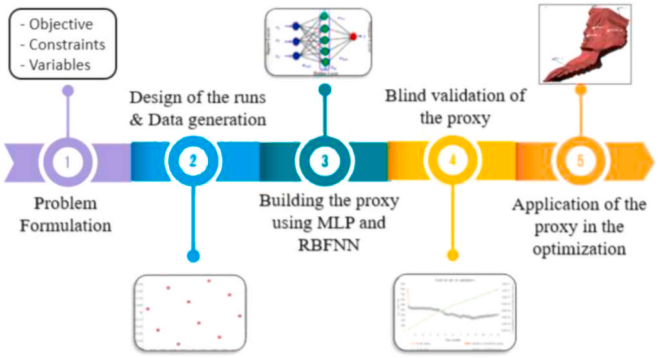

Fig. 2. Flowchart of the main steps of the work.

Table 5
Performance analysis of MLP-LMA proxy model.

Phase	Parameters	AARD (%) (runs)		
		Min	Avg.	Max
Training	FOPR	0.12	0.23	0.37
	FOPT $(t)_{final}$	0.0076	0.03	0.14
	FWPR	0.49	1.29	5.13
	FWPT $(t)_{final}$	0.001	0.32	3.03
	FWCT	0.42	1.53	4.23
	FPR	0.001	0.013	0.017
Validation (blind runs)	FOPR	1.22	1.48	2.10
	FOPT $(t)_{final}$	0.17	0.25	0.46
	FWPR	2.72	3.52	5.34
	FWPT $(t)_{final}$	1.57	2.14	3.42
	FWCT	2.33	2.78	3.32
	FPR	0.05	0.07	0.09

Table 6
Performance analysis of RBFNN-ACO proxy model.

Phase	Parameters	AARD (%) (runs)		
		Min	Avg.	Max
Training	FOPR	0.17	0.73	1.03
	FOPT $(t)_{final}$	0.05	0.19	0.41
	FWPR	0.98	1.84	6.37
	FWPT $(t)_{final}$	0.12	1.05	4.88
	FWCT	0.93	2.37	5.69
	FPR	0.009	0.08	0.13
Validation (blind runs)	FOPR	1.29	1.55	3.16
	FOPT $(t)_{final}$	0.34	0.61	1.13
	FWPR	2.93	4.18	6.68
	FWPT $(t)_{final}$	1.84	2.91	4.28
	FWCT	2.76	3.07	4.33
	FPR	0.05	0.11	0.15

Table 7
Performance analysis of RBFNN-GWO proxy model.

Phase	Parameters	AARD (%) (runs)		
		Min	Avg.	Max
Training	FOPR	0.16	0.64	0.96
	FOPT $(t)_{final}$	0.04	0.11	0.33
	FWPR	0.93	1.72	6.31
	FWPT $(t)_{final}$	0.09	1.03	4.80
	FWCT	0.90	2.15	5.26
	FPR	0.009	0.06	0.10
Validation (blind runs)	FOPR	1.28	1.51	3.03
	FOPT $(t)_{final}$	0.31	0.55	1.09
	FWPR	2.92	4.14	6.63
	FWPT $(t)_{final}$	1.73	2.80	4.22
	FWCT	2.71	3.00	4.28
	FPR	0.04	0.10	0.15

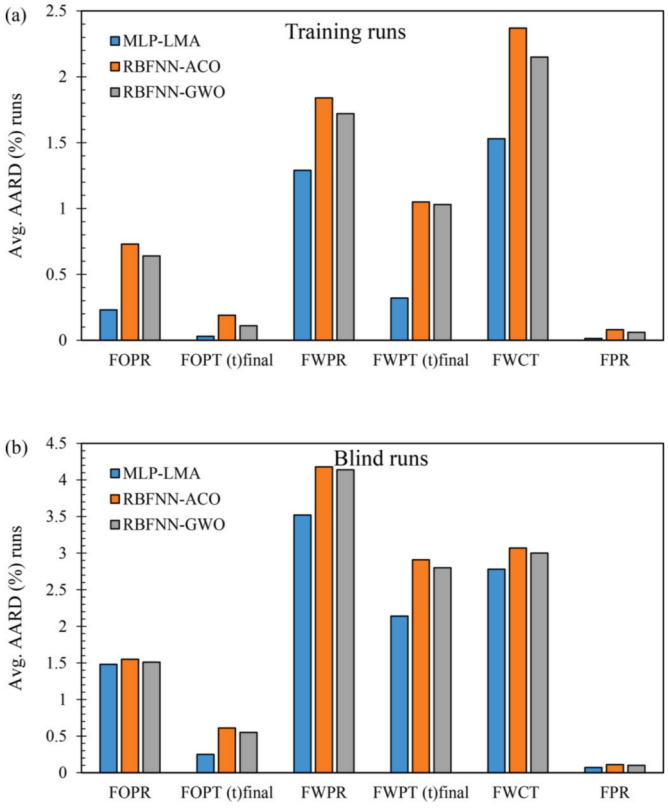

Fig. 3. Comparison between the performance of the established proxy models for predicting the different needed parameters of: (a) training runs and (b) blind runs.

$$FWCT\left(t, q_{injw}, q_{injg}, half_{cycg-w}, downtime\right) = \frac{FWPR\left(t, q_{injw}, q_{injg}, half_{cycg-w}, downtime\right)}{FOPR\left(t, q_{injw}, q_{injg}, half_{cycg-w}, downtime\right) + FWPR\left(t, q_{injw}, q_{injg}, half_{cycg-w}, downtime\right)} \quad (19)$$

In the above equation, FOPR and FWPR refer to the field oil and water production rates, respectively.

5. Implementation procedure

Two types of proxy models were created to estimate all the included parameters in the formulated optimization problem (*FOPR*, *FWPR*, *FPR*) based on MLP and RBFNN, while the other parameters (*FOPT*, *FWCT*) are evaluated based on the rates and time. As mentioned in the previous sections, MLP model was optimized using LM algorithm (the weights and bias), and trial & error technique was applied for investigating its proper topologies (activation functions, number of hidden layers and their associated neurons), while the parameters of RBFNN paradigm were optimized using ACO and GWO. The control parameters of ACO

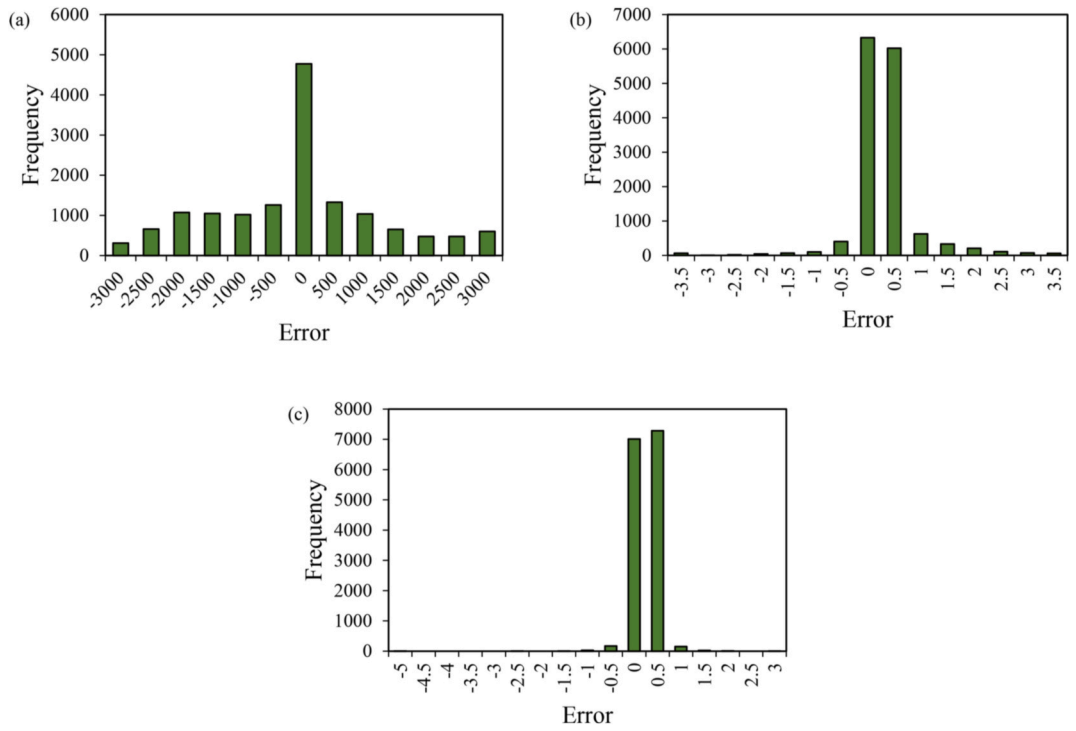

Fig. 4. Distribution of the errors associated with MLP-LMA proxy during the training phase: (a) FOPT, (b) FPR, and (c) FWCT.

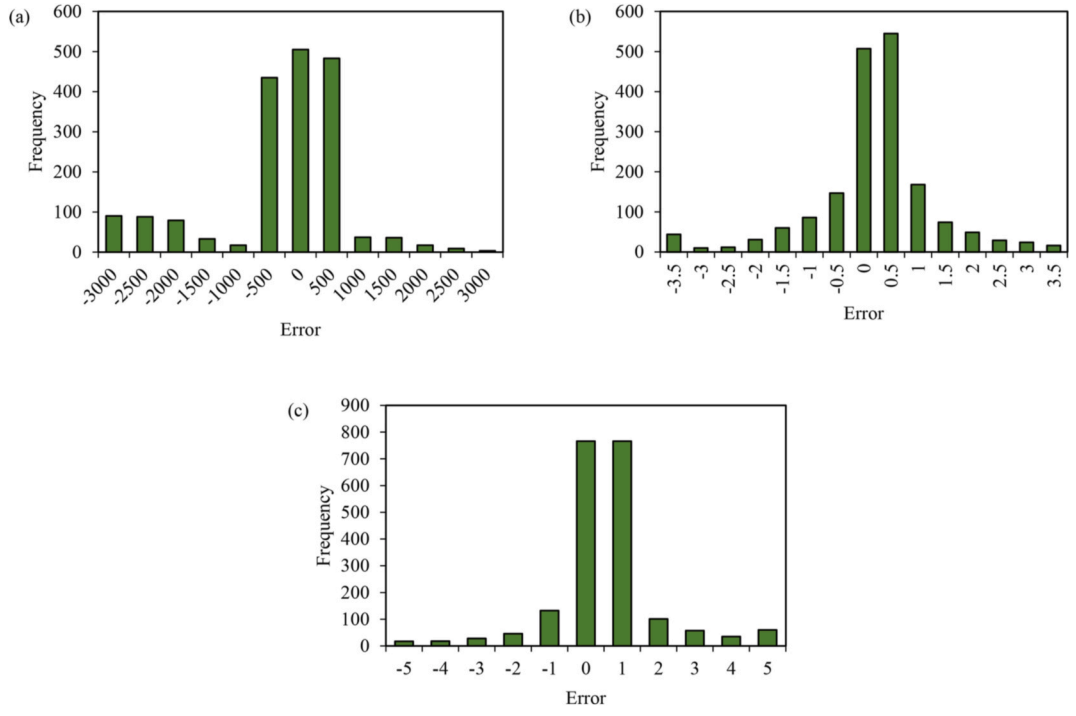

Fig. 5. Distribution of the errors associated with MLP-LMA proxy during the blind validation phase: (a) FOPT, (b) FPR, and (c) FWCT.

and GWO are reported in Table 4.

To build these proxy models, 24 runs for each of the downtime levels were selected, thus 72 runs were considered in the building phase of the proxy models. Latin Hypercube Design (LHD) was used for attributing the half cycle time and gas and water injection rates to these runs. Then, these latter were simulated using Eclipse 300. Afterwards, the generated database was used to develop the proxy models. Besides, 10 supplementary runs were selected randomly as blind runs for testifying the performances of the proxy models for unseen scenarios.

In the last step of the implementation, the best proxy elaborated using the aforesaid machine learning techniques was coupled with ACO and GWO to find the proper design parameters of the formulated WAG optimization problem. Fig. 2 summarizes the main steps of the work.

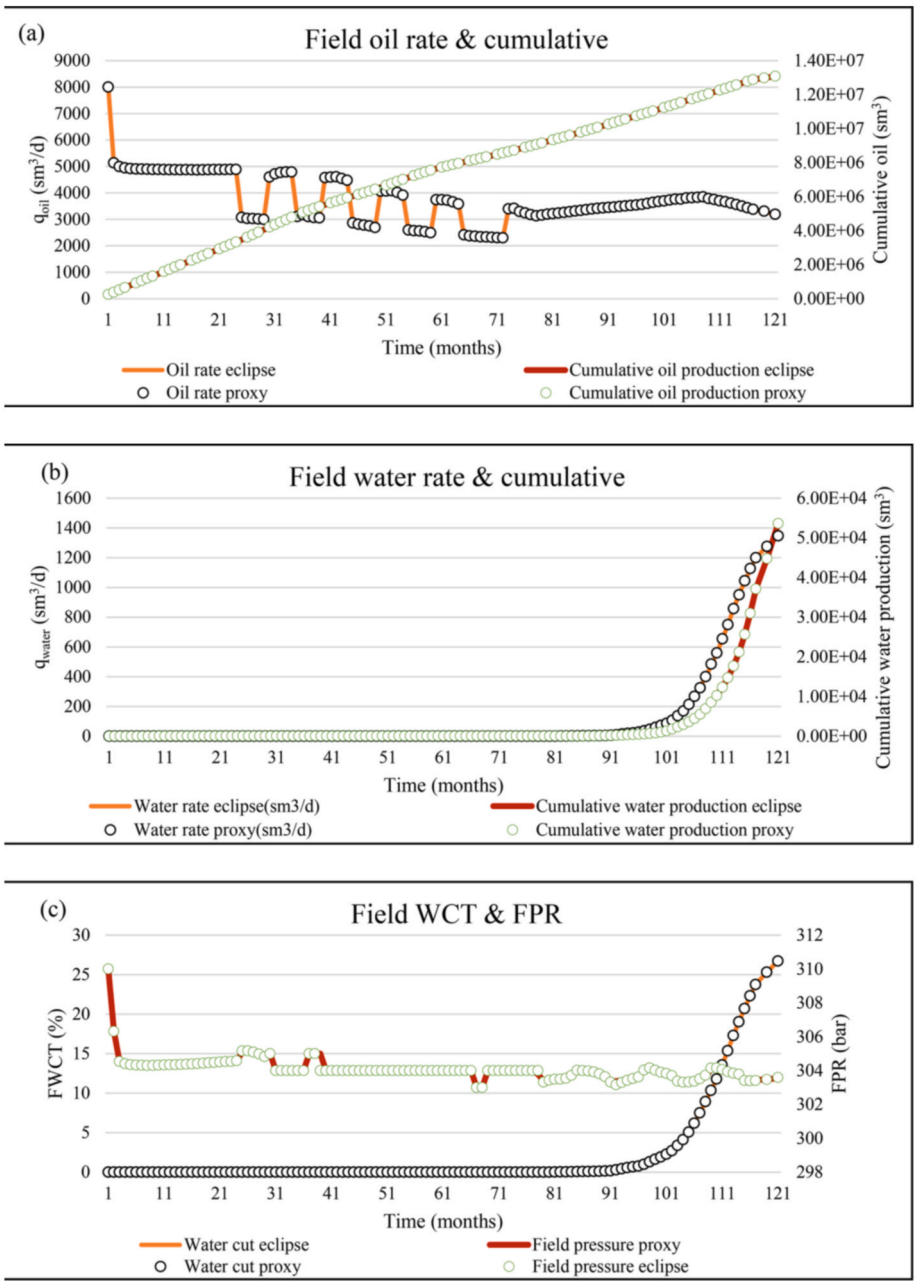

Fig. 6. Demonstration of the reliability of the MLP-LMA proxy model to emulate the outcomes of a run included in the training phase (a) FOPR and FOPT (b) FWPR and FWPT (c) FWCT and FPR.

6. Results and discussion

Before displaying the main findings of the proposed workflow for optimizing the WAG process using the hybridization SC-nature-inspired algorithms, it is worth mentioning that the performance evaluation of the training and blind validation steps was carried out using statistical and graphical error analysis. Average absolute relative deviation (AARD %) was applied as the main index to examine the reliability of the proxy. This index is expressed as:

$$AARD\% = \frac{1}{N}\sum_{j=1}^{N}\left|\frac{T_{j_E} - O_{j_P}}{T_{j_E}}\right| \times 100 \tag{20}$$

where the outputs of the commercial simulator and the proxy are denoted by T_E and O_P, respectively, and N represents the number of points.

Tables 5–7 show the performance analysis of the different proxy models (MLP-LMA, RBFNN-ACO, and RBFNN-GWO) during the learning (construction) and validation phases. In these tables, the errors (AARD) associated with each parameter involved in the optimization of the studied WAG process are reported. In this regard, three kinds of AARD, including the average, minimum, and maximum values, are reported with respect to the considered 72 runs and the 10 blind runs. Besides, the bar plots (a) and (b) of Fig. 3 display a visual comparison between the performance of the established proxy paradigms for estimating the investigated parameters of the training and blind runs, respectively. Based on the performances exhibited, the proposed proxy models can accurately predict the different parameters required in the optimization problem. In addition, a comparison of the AARD achieved by each of the models (for different parameters) suggests that MLP-LMA proxy outperforms the other two proxy paradigms. Therefore, MLP-LMA proxy model is selected for further evaluation and optimization.

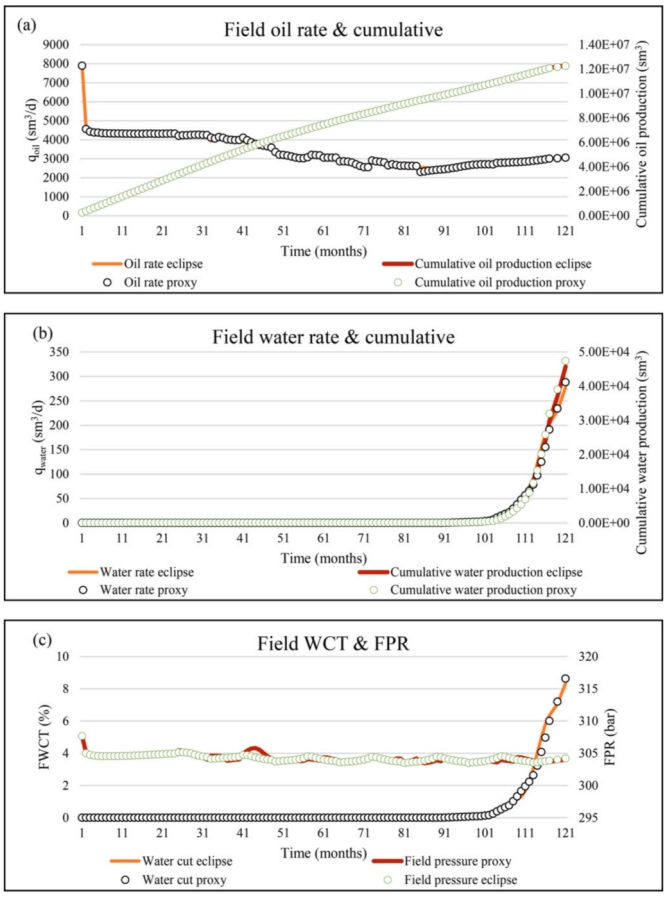

Fig. 7. Demonstration of the reliability of the MLP-LMA proxy model to emulate the outcomes of one blind run (a) FOPR and FOPT (b) FWPR and FWPT (c) FWCT and FPR.

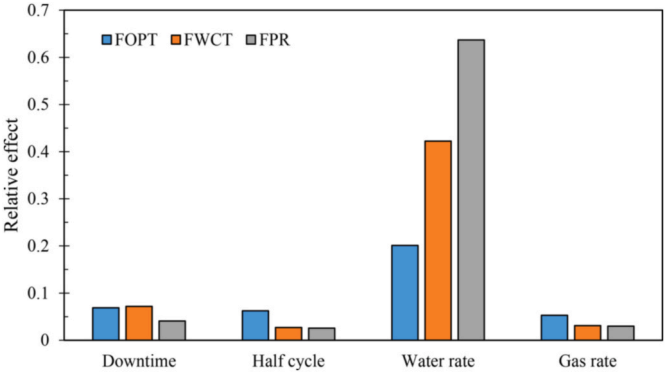

Fig. 8. Relative importance of the main input variables on the outputs of the proxy.

In order to test the reliability of the best proxy model, Figs. 4 and 5 illustrate the distributions of the errors between the outputs of the commercial simulators and MLP-LMA proxy in histogram diagrams for the main parameters of the formulated problem during the training and blind validation steps, respectively. As graphically shown in these figures, a normal distribution of the errors with a center equal to or very close to zero-error value is noticed in all the investigated parameters during the training and blind validation steps. This confirms again the high robustness of the suggested proxy model.

In another step, the reliability of the implemented MLP-LMA proxy model was tested for predicting the different parameters as a function of time. Figs. 6 and 7 compare the results emulated by the implemented best-proxy and those of the numerical simulator for a run included in the learning phase and for a blind run, respectively. In all the graphs, the parameters are represented as a function of time.

According to the exhibited results, the proposed MLP-LMA proxy model has a strong ability to correctly estimate the different parameters needed in optimization, either included in the learning or the blind phase. Also, very small errors were marked with all parameters. As a result, the performance of the developed dynamic proxy model is very satisfactory, and therefore this paradigm can be used in the task of WAG process optimization for the K1/K2 segment. Besides, it can be deduced from these figures that the trend of the outputs of the proxy is very similar to that of the numerical simulator. For example, subplot (a) of Figs. 6 and 7 reveals that the proxy captured the macroscopic and microscopic effects by injecting water (relatively high FOPR during the half cycles of water and after the downtime of the process) and gas

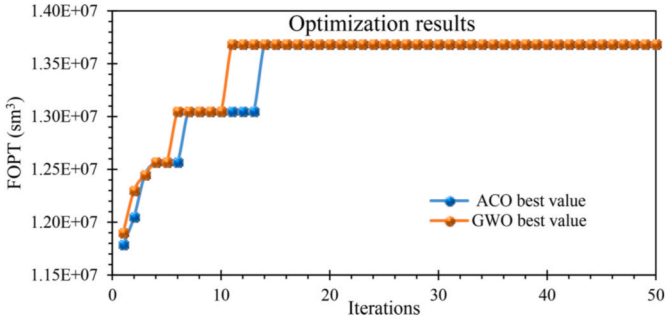

Fig. 9. Optimization results with the proposed hybridizations: proxy-ACO and proxy-GWO.

Table 9
Comparison of the results of the proxy model and the numerical simulator for the best scenario.

Parameter	Proxy run (for best GF[a] parameters)	Eclipse 300 run (for best GF parameters)	AARD (%)
$FOPT_{t\_final}$ (sm^3)	13,685,903	13,654,497	0.23
FWCT (%)	–	–	2.37
FPR (bar)	–	–	0.08

[a] Global Function.

Table 8
Summary of the best results achieved.

Algorithm	Number of iterations to reach best FOPT	Best FOPT (10^6 sm^3)	q_{injw} (sm^3/d) (best FOPT)	q_{injg} (sm^3/d) (best FOPT)	$half_{cycg-w}$ (month) (best FOPT)	WAG Ratio	Slug size (PV)	Down time (years)	Max WCT (%)	Min and Max FPR (bar)
ACO	14	13.68	5652	10^6	6	1.98	0.04	3	35.42	305–310
GWO	11	13.68	5652	10^6	6	1.98	0.04	3	35.42	305–310

(relatively low FOPR during the half cycles of gas), respectively. Also, subplots (b) and (c) of Figs. 6 and 7 demonstrate that the downtime results in the increase in FWPR and FWCT, while the pressure is almost stable.

To examine the relative importance of the main input parameters on the main outputs of the smart models needed in the optimization step, the relevancy factor (r) was applied. The higher the absolute value of r, the more the effect of this parameter on the output. The mathematical formula of this factor is expressed as follows (Chen et al., 2014; Nait Amar, 2020):

$$r(I_j,\ O) = \frac{\sum_{i=1}^{N}\left(I_{j,i} - \overline{I}_j\right)\left(O_i - \overline{O}\right)}{\sqrt{\sum_{i=1}^{N}\left(I_{j,i} - \overline{I}_j\right)^2 \sum_{i=1}^{n}\left(O_i - \overline{O}\right)^2}} \tag{21}$$

In the above equation, the index of the point is denoted i; I_j represents the jth input,$\overline{I}_j$ points out the average value of I_j, O and $\overline{O}$ are the proxy output value and its average, respectively. As depicted in Fig. 8, water injection rate has the highest impact on the main outputs of the suggested proxy model.

After confirming the reliability of MLP-LMA proxy model, it was coupled with ACO and GWO in order to find the proper design parameters with respect to equation (18) that illustrates the mathematical formulation of the WAG optimization problem. The design parameters include water injection rate, gas injection rate, half-cycle time, and the downtime (WAG ratio and slug size are deduced from the other parameters).

The results obtained with the two hybridizations, namely proxy-ACO and proxy-GWO, are presented in Table 8 and in Fig. 9.

According to the reported results, it can be noted that the optimization parameters found by the proxy-metaheuristic hybridizations are the same with only a slight difference in the convergence speed, where only 11 iterations were taken by GWO to find the optimum, while ACO used 14 iterations for this purpose.

In order to validate the robustness of the developed proxy paradigm, the outputs of the dynamic proxy corresponding to the best control parameters found with the two hybridizations are compared with those from the numerical simulator. The suitable control parameters found using the direct simulation (commercial simulator) were the same as those mentioned in Table 8. However, the AARD associated with predictions of the proposed proxy versus the direct simulation are shown in Table 9.

As seen in Table 9, very good match between the results of the MLP-LMA proxy model and the numerical simulator is obtained, where very small errors are observed (for all the parameters) for the best run found. This confirms the precision and robustness of the optimization procedure presented in this study. Furthermore, and from the simulation time perspective, it is worth mentioning that by using an Intel® CoreTM i7-7700HQ 2.80 GHz and 16 Gb of RAM, our suggested proxy takes only 1.2 s to generate the whole needed parameters for one realization, while more than 15 min is required using the commercial simulator. This significant reduction in the simulation time demonstrates the robustness and the efficiency of the proposed proxy.

The optimization results show that a field water rate of 5652 sm^3/d and a field gas rate of 10^6 sm^3/d with an injection half-cycle of 6 months and a downtime of 3 years are the optimal parameters for the WAG process studied in this paper.

To end with, it is needed to mention that the findings gained from this study contribute to the knowledge of the mathematics of oil recovery, specifically EOR techniques based on gas injection, from many standing points of view, viz. the implementation of simple-to-use and robust time-dependent proxy models for real geological fields, the optimization of WAG process under dynamic constraints, and also the ability of the nature-inspired algorithms for resolving the optimization problems related to EOR techniques. The work carried out and the achieved outcomes offer very interesting recommendations for future works such as the development of proxy models for hybrid EOR schemes and the mono/multi-objective optimization of more complicated EOR methods. Finally, it is important to add that the suggested proxy scheme can be considered as a substitution of the direct simulation for WAG projects which are similar to the case studied in this investigation if the design parameters are within the considered ranges. This ensures the satisfaction of the applicability conditions of the proxy, thus, accurate predictions are expected as the main sources of errors are resulted from the disruption of these conditions.

7. Conclusions

In this paper, we applied a hybridization of intelligent techniques for optimizing a WAG process in a real field (K1/K2 segment of Gullfaks). The aim of the study was to maximize the total oil production associated with this project in the presence of dynamic technical constraints. Robust dynamic proxy models were built with two types of artificial neural networks, viz. MLP and RBFNN. Based on the achieved results, the following conclusions can be drawn:

1. The proposed proxy models can emulate accurately the outputs of the commercial simulator.
2. MLP-LMA proxy outperformed the other two proxy models.
3. The best dynamic proxy hybridizations developed with ACO and GWO provide the optimal parameters for WAG control, including water and gas injection rates, injection half-cycle, downtime, WAG ratio and gas slug size.
4. The suggested proxy model ensured significantly reducing the simulation time and conserving the required accuracy.
5. The obtained results confirmed the performance of the suggested methodology for a real reservoir.

Author contributions

Menad Nait Amar: Data curation, Formal analysis, Methodology, Investigation and Modelling, Software, Writing. Ashkan Jahanbani Ghahfarokhi: Supervision, Methodology, Writing – review & editing. Cuthbert Shang Wui Ng: Writing – review & editing. Noureddine Zeraibi: Supervision, Methodology, Reviewing and Editing.

Declaration of competing interest

The authors declare that they have no known competing financial interests or personal relationships that could have appeared to influence the work reported in this paper.

Acknowledgment

The authors thank Mr. D Aqnan Marusaha Matthew at Department of Geoscience and Petroleum, Norwegian University of Science and Technology for providing the high-resolution figures regarding the main characteristics of the Gullfaks, segment K1/K2.

Nomenclature

AARD	Average Absolute Relative Deviation
ACO	Ant Colony Optimization
EOR	Enhanced Oil Recovery
LHD	Latin Hypercube Design
FOPR	Field Oil Production Rate
FOPT	Field Oil Production Total
FPR	Field Pressure
FWCT	Field Water Cut
FWPR	Field Water Production Rate
FWPT	Field Water Production Total

FWIR	Field Water Injection Rate
GWO	Grey Wolf Optimization
LM	Levenberg–Marquardt Algorithm
MLP	Multi-layer Perceptron
MMP	Minimum Miscibility Pressure
q_{injw}	Field Water Injection Rate
q_{injg}	Field Gas Injection Rate
RBFNN	Radial Basis Function Neural Network
WAG	Water Alternating Gas

References

Afzali, S., Ghamartale, A., Rezaei, N., Zendehboudi, S., 2020. Mathematical modeling and simulation of water-alternating-gas (WAG) process by incorporating capillary pressure and hysteresis effects. Fuel 263, 116362.

Afzali, S., Rezaei, N., Zendehboudi, S., 2018. A comprehensive review on enhanced oil recovery by water alternating gas (WAG) injection. Fuel 227, 218–246.

Ahmadi, M.A., Shadizadeh, S.R., 2013. Implementation of a high-performance surfactant for enhanced oil recovery from carbonate reservoirs. J. Petrol. Sci. Eng. 110, 66–73.

Ahmadi, M.A., Zendehboudi, S., James, L.A., 2018. Developing a robust proxy model of CO 2 injection: coupling Box–Behnken design and a connectionist method. Fuel 215, 904–914.

Ahmed, T., 2018. Reservoir Engineering Handbook. Gulf professional publishing.

Amooie, M.A., Hemmati-Sarapardeh, A., Karan, K., Husein, M.M., Soltanian, M.R., Dabir, B., 2019. Data-driven modeling of interfacial tension in impure CO2-brine systems with implications for geological carbon storage. Int. J. Greenh. Gas Contr. 90, 102811.

Bakyani, A.E., Sahebi, H., Ghiasi, M.M., Mirjordavi, N., Esmaeilzadeh, F., Lee, M., Bahadori, A., 2016. Prediction of CO2–oil molecular diffusion using adaptive neuro-fuzzy inference system and particle swarm optimization technique. Fuel 181, 178–187.

Baldwin, J.L., Bateman, R.M., Wheatley, C.L., others, 1990. Application of a neural network to the problem of mineral identification from well logs. Log. Anal. 31.

Belazreg, L., Mahmood, S.M., 2020. Water alternating gas incremental recovery factor prediction and WAG pilot lessons learned. J. Pet. Explor. Prod. Technol. https://doi.org/10.1007/s13202-019-0694-x.

Belazreg, L., Mahmood, S.M., Aulia, A., 2020. Random forest algorithm for co2 water alternating gas incremental recovery factor prediction. Int. J. Adv. Sci. Technol.

Belazreg, L., Mahmood, S.M., Aulia, A., 2019. Novel approach for predicting water alternating gas injection recovery factor. J. Pet. Explor. Prod. Technol. https://doi.org/10.1007/s13202-019-0673-2.

Benamara, C., Gharbi, K., Nait Amar, M., Hamada, B., 2020. Prediction of wax appearance temperature using artificial intelligent techniques. Arabian J. Sci. Eng. 45, 1319–1330. https://doi.org/10.1007/s13369-019-04290-y.

Bian, X.-Q., Huang, J.-H., Wang, Y., Liu, Y.-B., Kaushika Kasthuriarachchi, D.T., Huang, L.-J., 2019. Prediction of wax disappearance temperature by intelligent models. Energy Fuel. 33, 2934–2949.

Bian, X.-Q., Song, Y.-L., Mwamukonda, M.K., Fu, Y., 2020. Prediction of the sulfur solubility in pure H2S and sour gas by intelligent models. J. Mol. Liq. 299, 112242.

Bian, X.-Q., Zhang, L., Du, Z.-M., Chen, J., Zhang, J.-Y., 2018. Prediction of sulfur solubility in supercritical sour gases using grey wolf optimizer-based support vector machine. J. Mol. Liq. 261, 431–438.

Blum, C., 2005. Ant colony optimization: introduction and recent trends. Phys. Life Rev. 2, 353–373.

Chen, G., Fu, K., Liang, Z., Sema, T., Li, C., Tontiwachwuthikul, P., Idem, R., 2014. The genetic algorithm based back propagation neural network for MMP prediction in CO2-EOR process. Fuel 126, 202–212.

Christensen, J.R., Stenby, E.H., Skauge, A., 2001. Review of WAG field experience. SPE Reservoir Eval. Eng. 4, 97–106.

Daryasafar, A., Keykhosravi, A., Shahbazi, K., 2019. Modeling CO2 wettability behavior at the interface of brine/CO2/mineral: application to CO2 geo-sequestration. J. Clean. Prod. 239, 118101. https://doi.org/10.1016/j.jclepro.2019.118101.

Ghiasi, M.M., Mohammadi, A.H., 2015. Development of reliable models for determination of required monoethanolamine (MEA) circulation rate in amine plants. Separ. Sci. Technol. 50, 2248–2256.

Ghiasi, M.M., Shahdi, A., Barati, P., Arabloo, M., 2014. Robust modeling approach for estimation of compressibility factor in retrograde gas condensate systems. Ind. \& Eng. Chem. Res. 53, 12872–12887.

Haykin, S., 2010. Neural Networks and Learning Machines, vol. 3. E. Pearson Education India.

Hemmati-Sarapardeh, A., Alipour-Yeganeh-Marand, R., Naseri, A., Safiabadi, A., Gharagheizi, F., Ilani-Kashkouli, P., Mohammadi, A.H., 2013. Asphaltene precipitation due to natural depletion of reservoir: determination using a SARA fraction based intelligent model. Fluid Phase Equilib 354, 177–184.

Hemmati-Sarapardeh, A., Dabir, B., Ahmadi, M., Mohammadi, A.H., Husein, M.M., 2019. Modelling asphaltene precipitation titration data: a committee of machines and a group method of data handling. Can. J. Chem. Eng. 97, 431–441.

Hemmati-Sarapardeh, A., Ghazanfari, M.-H., Ayatollahi, S., Masihi, M., 2016. Accurate determination of the CO2-crude oil minimum miscibility pressure of pure and impure CO2 streams: a robust modelling approach. Can. J. Chem. Eng. 94, 253–261.

Hemmati-Sarapardeh, A., Varamesh, A., Husein, M.M., Karan, K., 2018. On the evaluation of the viscosity of nanofluid systems: modeling and data assessment. Renew. Sustain. Energy Rev. 81, 313–329.

Hemmati Sarapardeh, A., Larestani, A., Nait Amar, M., Hajirezaie, S., 2020. Applications of Artificial Intelligence Techniques in the Petroleum Industry. Gulf Professional Publishing.

Heris, S.M.K., Khaloozadeh, H., 2014. Ant colony estimator: an intelligent particle filter based on. ACOR. Eng. Appl. Artif. Intell. 28, 78–85.

Jaber, A.K., Awang, M.B., Lenn, C.P., 2017. Box-Behnken design for assessment proxy model of miscible CO2-WAG in heterogeneous clastic reservoir. J. Nat. Gas Sci. Eng. 40, 236–248.

Kamari, A., Bahadori, A., Mohammadi, A.H., Zendehboudi, S., 2014. Evaluating the unloading gradient pressure in continuous gas-lift systems during petroleum production operations. Pet. Sci. Technol. 32, 2961–2968.

Karkevandi-Talkhooncheh, A., Rostami, A., Hemmati-Sarapardeh, A., Ahmadi, M., Husein, M.M., Dabir, B., 2018. Modeling minimum miscibility pressure during pure and impure CO2 flooding using hybrid of radial basis function neural network and evolutionary techniques. Fuel 220, 270–282.

Killough, J.E., Kossack, C.A., others, 1987. Fifth comparative solution project: evaluation of miscible flood simulators. In: SPE Symposium on Reservoir Simulation.

Kulkarni, M.M., Rao, D.N., 2005. Experimental investigation of miscible and immiscible Water-Alternating-Gas (WAG) process performance. J. Pet. Sci. Eng. 48, 1–20.

Lake, L.W., Johns, R., Rossen, B., Pope, G.A., others, 2014. Fundamentals of Enhanced Oil Recovery.

Mirjalili, S., Mirjalili, S.M., Lewis, A., 2014. Grey wolf optimizer. Adv. Eng. Softw. https://doi.org/10.1016/j.advengsoft.2013.12.007.

Mohaghegh, S.D., 2017. Data-Driven Reservoir Modeling. Society of Petroleum Engineers.

Mohagheghian, E., James, L.A., Haynes, R.D., 2018. Optimization of hydrocarbon water alternating gas in the Norne field: application of evolutionary algorithms. Fuel 223, 86–98.

Nait Amar, M., 2021. Prediction of hydrate formation temperature using gene expression programming. J. Nat. Gas Sci. Eng. 89, 103879. https://doi.org/10.1016/j.jngse.2021.103879.

Nait Amar, M., 2020. Modeling solubility of sulfur in pure hydrogen sulfide and sour gas mixtures using rigorous machine learning methods. Int. J. Hydrogen Energy 45, 33274–33287. https://doi.org/10.1016/j.ijhydene.2020.09.145.

Nait Amar, M., Ghriga, M.A., Ouaer, H., 2021. On the evaluation of solubility of hydrogen sulfide in ionic liquids using advanced committee machine intelligent systems. J. Taiwan Inst. Chem. Eng. 118, 159–168. https://doi.org/10.1016/j.jtice.2021.01.007.

Nait Amar, M., Jahanbani Ghahfarokhi, A., Zeraibi, N., 2020a. Predicting thermal conductivity of carbon dioxide using group of data-driven models. J. Taiwan Inst. Chem. Eng. 113, 165–177. https://doi.org/10.1016/j.jtice.2020.08.001.

Nait Amar, M., Zeraibi, N., 2019. An efficient methodology for multi-objective optimization of water alternating CO2 EOR process. J. Taiwan Inst. Chem. Eng. 99, 154–165. https://doi.org/10.1016/j.jtice.2019.03.016.

Nait Amar, M., Zeraibi, N., Jahanbani Ghahfarokhi, A., 2020b. Applying hybrid support vector regression and genetic algorithm to water alternating CO2 gas EOR. Greenh. Gases Sci. Technol. 10, 613–630. https://doi.org/10.1002/ghg.1982.

Nait Amar, M., Zeraibi, N., Redouane, K., 2018a. Optimization of WAG process using dynamic proxy, genetic algorithm and ant colony optimization. Arab. J. Sci. Eng. 43, 6399–6412. https://doi.org/10.1007/s13369-018-3173-7.

Nait Amar, M., Zeraibi, N., Redouane, K., 2018b. Bottom hole pressure estimation using hybridization neural networks and grey wolves optimization. Petroleum 4, 419–429. https://doi.org/10.1016/j.petlm.2018.03.013.

Nwachukwu, A., Jeong, H., Sun, A., Pyrcz, M., Lake, L.W., 2018. Machine learning-based optimization of well locations and WAG parameters under geologic uncertainty. In: Proceedings - SPE Symposium on Improved Oil Recovery. https://doi.org/10.2118/190239-ms.

Panjalizadeh, H., Alizadeh, A., Ghazanfari, M., Alizadeh, N., 2015. Optimization of the WAG injection process. Pet. Sci. Technol. 33, 294–301.

Ranaee, E., Inzoli, F., Riva, M., Guadagnini, A., 2019. Hysteresis effects of three-phase relative permeabilities on black-oil reservoir simulation under WAG injection protocols. J. Pet. Sci. Eng. 176, 1161–1174.

Rashid, S., Harimi, B., Hamidpour, E., 2017. Prediction of CO2-Brine interfacial tension using a rigorous approach. J. Nat. Gas Sci. Eng. 45, 108–117.

Shpak, R., 2013. Modeling of miscible WAG injection using real geological field data. In: Institutet for Petroleumsteknologi Og Anvendt Geofysikk.

Siddique, N., Adeli, H., 2013. Computational Intelligence: Synergies of Fuzzy Logic, Neural Networks and Evolutionary Computing. John Wiley & Sons.

Socha, K., Dorigo, M., 2008. Ant colony optimization for continuous domains. Eur. J. Oper. Res. 185, 1155–1173.

Tatar, A., Naseri, S., Bahadori, M., Hezave, A.Z., Kashiwao, T., Bahadori, A., Darvish, H., 2016. Prediction of carbon dioxide solubility in ionic liquids using MLP and radial basis function (RBF) neural networks. J. Taiwan Inst. Chem. Eng. 60, 151–164.

Tatar, A., Naseri, S., Sirach, N., Lee, M., Bahadori, A., 2015. Prediction of reservoir brine properties using radial basis function (RBF) neural network. Petroleum 1, 349–357. https://doi.org/10.1016/j.petlm.2015.10.011.

Tillerson, R.W., 2008. Meeting global energy supply and demand challenges. In: 19th World Petroleum Congress.

Varamesh, A., Hemmati-Sarapardeh, A., Dabir, B., Mohammadi, A.H., 2017a. Development of robust generalized models for estimating the normal boiling points of pure chemical compounds. J. Mol. Liq. 242, 59–69.

Varamesh, A., Hemmati-Sarapardeh, A., Moraveji, M.K., Mohammadi, A.H., 2017b. Generalized models for predicting the critical properties of pure chemical compounds. J. Mol. Liq. 240, 777–793.

Whitson, C.H., Brulé, M.R., others, 2000. Phase Behavior. Henry L. Doherty Memorial Fund of AIME, Society of Petroleum Engineers Richardson, TX.

Yousef, A.M., Kavousi, G.P., Alnuaimi, M., Alatrach, Y., 2020. Predictive data analytics application for enhanced oil recovery in a mature field in the Middle East. Pet. Explor. Dev. https://doi.org/10.1016/S1876-3804(20)60056-8.

Zendehboudi, S., Rezaei, N., Lohi, A., 2018. Applications of hybrid models in chemical, petroleum, and energy systems: a systematic review. Appl. Energy 228, 2539–2566.

Zhang, Y., Lu, R., Forouzanfar, F., Reynolds, A.C., 2017. Well placement and control optimization for WAG/SAG processes using ensemble-based method. Comput. Chem. Eng. 101, 193–209.

Zhao, N., Wen, X., Yang, J., Li, S., Wang, Z., 2015. Modeling and prediction of viscosity of water-based nanofluids by radial basis function neural networks. Powder Technol 281, 173–183.